NeuroImage 84 (2014) 733–741

Contents lists available at ScienceDirect

NeuroImage

journal homepage: www.elsevier.com/locate/ynimg

In vitro and in vivo evaluation of ^{11}C-SD5024, a novel PET radioligand for human brain imaging of cannabinoid CB_1 receptors ☆

Tetsuya Tsujikawa [a], Sami S. Zoghbi [a], Jinsoo Hong [a], Sean R. Donohue [a], Kimberly J. Jenko [a], Robert L. Gladding [a], Christer Halldin [b], Victor W. Pike [a], Robert B. Innis [a], Masahiro Fujita [a,*]

[a] Molecular Imaging Branch, National Institute of Mental Health, National Institutes of Health, Bethesda, MD, USA
[b] Karolinska Institutet, Department of Clinical Neuroscience, Psychiatry Section, Stockholm, Sweden

ARTICLE INFO

Article history:
Accepted 18 September 2013
Available online 25 September 2013

Keywords:
CB_1 receptors
Cannabinoid
PET
Receptor imaging

ABSTRACT

We recently developed a novel cannabinoid subtype-1 (CB_1) receptor radioligand ^{11}C-SD5024 for brain imaging. This study aimed to evaluate ^{11}C-SD5024 both in vitro and in vivo and compare it with the other CB_1 receptor ligands previously used in humans, i.e., ^{11}C-MePPEP, ^{11}C-OMAR, ^{18}F-MK-9470, and ^{18}F-FMPEP-d_2. In vitro experiments were performed to measure dissociation constant (K_i) in the human brain and to measure the lipophilicity of the five CB_1 receptor ligands listed above. In vivo specific binding in monkeys was measured by comparing total distribution volume (V_T) at baseline and after full receptor blockade. The kinetics of ^{11}C-SD5024 in humans were evaluated in seven healthy subjects with compartmental modeling. SD5024 showed $K_i = 0.47$ nM, which was at an intermediate level among the five CB_1 receptor ligands. Lipophilicity ($LogD_{7.4}$) was 3.79, which is appropriate for brain imaging. Monkey scans showed high proportion of specific binding: ~80% of V_T. In humans, ^{11}C-SD5024 showed peak brain uptake of 1.5–3 standardized uptake value, which was slightly higher than that of ^{11}C-OMAR and ^{18}F-MK-9470. One-compartment model showed good fitting, consistent with the vast majority of brain uptake being specific binding found in the monkey. Regional V_T values were consistent with known distribution of CB_1 receptors. V_T calculated from 80 and 120 min of scan data was strongly correlated ($R^2 = 0.97$), indicating that 80 min provided adequate information for quantitation and that the influence of radiometabolites was low. Intersubject variability for V_T of ^{11}C-SD5024 was 22%, which was low among the five radioligands and indicated precise measurement. In conclusion, ^{11}C-SD5024 has appropriate affinity and lipophilicity, high specific binding, moderate brain uptake, and provides good precision to measure the binding. The results suggest that ^{11}C-SD5024 is slightly better than or equivalent to ^{11}C-OMAR and that both are suitable for clinical studies, especially those that involve two scans in one day.

Published by Elsevier Inc.

Introduction

The cannabinoid type 1 (CB_1) receptor, which is one of the most abundant G protein-coupled receptors in the brain (Katona and Freund, 2008; Matsuda et al., 1990; Wilson and Nicoll, 2002), is thought to have an important role in normal physiology (e.g., appetite and memory) and may be involved in the pathophysiology of some neuropsychiatric (schizophrenia) (Eggan et al., 2008) and metabolic (obesity) disorders (Gazzerro et al., 2007). In 2006, rimonabant, a CB_1 receptor inverse agonist was approved in Europe for appetite reduction and weight loss (Van Gaal et al., 2005). However, clinical research and/or use of two inverse agonists (rimonabant and taranabant) were discontinued in 2008 because of psychiatric side effects (depression, anxiety, and suicidal thoughts) (Jones, 2008). In these surroundings, a positron emission tomography (PET) radioligand for the CB_1 receptor that can provide reliable measurements of CB_1 receptor density and distribution in the brain could be one important means for understanding the complex role of the receptor and the many such disorders linked to it.

To image the CB_1 receptor in the human brain, four PET radioligands have mainly been used, ^{11}C-OMAR (^{11}C-JHU75528) (Wong et al., 2010), ^{18}F-MK-9470 (Burns et al., 2007; Sanabria-Bohórquez et al., 2010), ^{11}C-MePPEP (Terry et al., 2009) and ^{18}F-FMPEP-d_2 (Terry et al., 2010) (Fig. 1). Among these radioligands, ^{18}F-FMPEP-d_2 appears to be the one to provide the most precise measurement of the CB_1 receptor because of high peak brain uptake of ~6 standardized uptake value (SUV), a high percentage (85%) of specific binding in the monkey brain, small intersubject variability of total distribution volume (V_T) (26%), and a moderate level of retest variability (15%) (Terry et al., 2010).^{11}C-labeled ligands have some advantages over ^{18}F-labeled ones

☆ Disclosures: This study was supported by the Intramural Research Program of the National Institute of Mental Health, National Institutes of Health (IRP-NIMH-NIH) and by the 2011/2013 Wagner-Torizuka Fellowship of Society of Nuclear Medicine.

* Corresponding author at: Molecular Imaging Branch, National Institute of Mental Health, 10 Center Drive, Bethesda, MD 20892-1026, USA. Fax: +1 301 480 3610.
E-mail address: masahiro.fujita@nih.gov (M. Fujita).

1053-8119/$ – see front matter. Published by Elsevier Inc.
http://dx.doi.org/10.1016/j.neuroimage.2013.09.043

because the shorter half-life allows more than one synthesis per day using the same hot-cell and the lower radiation-absorbed doses allow more PET scans in each subject. On the other hand, the shorter half-life can make precise quantification difficult if radioligand kinetics are slow or if the concentrations in the brain and plasma are low.

Currently, no clearly good ^{11}C-labeled PET ligand is available to image the CB_1 receptor. Despite the high density of the CB_1 receptor, ^{11}C-OMAR shows peak brain uptake of only 1.5–2 SUV (Wong et al., 2010), which may make accurate quantification difficult. Although ^{11}C-MePPEP shows high peak brain uptake of 3–4 SUV, washout from brain is too slow for precise quantification possibly due to its high affinity. In addition, intersubject variability for V_T of ^{11}C-MePPEP is greater than 50% indicating poor precision of the measurement (Terry et al., 2009).

We recently developed a novel CB_1 receptor ligand labeled with ^{11}C from a 3,4-diarylpyrazoline structural class, namely ^{11}C-SD5024, [*cyano*-^{11}C](−)-3-(4-chlorophenyl)-*N*-[(4-cyanophenyl)sulfonyl]-4-phenyl-4,5-dihydro-1*H*-pyrazole-1-carboxamidine (Donohue et al., 2008) (Fig. 1). The purposes of this study were two folds, first, to evaluate both in vitro and in vivo the ability of ^{11}C-SD5024 to quantify CB_1 receptors, and second, to evaluate the utility of ^{11}C-SD5024 relative to other published ligands, particularly the ^{11}C-labeled ones. For these purposes, we measured in vitro affinity in human brain tissue and lipophilicity of all of the five ligands (SD5024, OMAR, MK-9470, MePPEP, and FMPEP-d_2), measured specific binding of ^{11}C-SD5024 in the monkey brain, and compared this with the specific binding of ^{11}C-MePPEP and ^{18}F-FMPEP-d_2 . In healthy humans, we measured the brain uptake and washout of ^{11}C-SD5024, calculated V_T and its intersubject variability as an indirect measure of the precision of the quantification, and compared these with the published results of the other four ligands. To image high density target such as CB_1 receptor using ^{11}C-labeled PET ligands, higher affinity is not necessarily better because slow washout from the brain of high affinity ligands makes quantification difficult. Appropriate lipophilicity for brain imaging is $LogD_{7.4}$ between 2 and 4 (Waterhouse, 2003). In brain scans, higher levels of specific binding and smaller intersubject variability are desired.

Material and methods

In vitro experiments

Binding assay

In vitro receptor binding assays were performed as previously described with minor modifications (Jenko et al., 2012). Briefly, the human parietal cortex was homogenized in buffer (20 mM HEPES, 5 mM $MgCl_2$, 1 mM EDTA, pH 7.4) with a Teflon pestle using a Glas-Col Homogenizing System and centrifuged at 25,000 ×*g* for 25 min at 4 °C. The pellet was re-suspended, aliquoted, and stored at −80 °C. Protein concentration was determined using the Bradford Protein Assay (Bio-Rad, Hercules, CA).

To determine the affinity (K_i and IC_{50}) of SD5024, MePPEP (PharmaCore, High Point, NC), FMPEP (Eli Lilly, Indianapolis, IN), OMAR (Johns Hopkins University, Baltimore, MD), and MK-9470 (Merck Research Laboratories, West Point, PA) for the CB_1 receptor, a heterologous binding assay was performed on one brain sample, in triplicate in each of two separate assays for a total $n = 6$. 100 μL of [^{3}H] MePPEP (specific activity 3.07 GBq/μmol; ~0.11 nM, diluted in buffer with 0.5% w/v BSA; Amersham GE Healthcare, UK) was added to each assay tube, followed by 100 μL of 12 concentrations (0.001 nM–3 μM) of the displacing ligand, 100 μL buffer (to determine total binding), or 1 μM rimonabant (Eli Lilly, Indianapolis, IN) (to determine non-specific binding). 800 μL of human parietal cortex suspension (41 μg/mL protein) was added and incubated for 90 min in a shaking water bath at 23 °C. Samples were filtered with a Brandel cell harvester (Gaithersburg, MD) through a Whatman GF/A filter paper, followed by three washes of 3 mL ice-cold 50 mM Tris–HCl buffer (pH = 7.4; 4 °C).

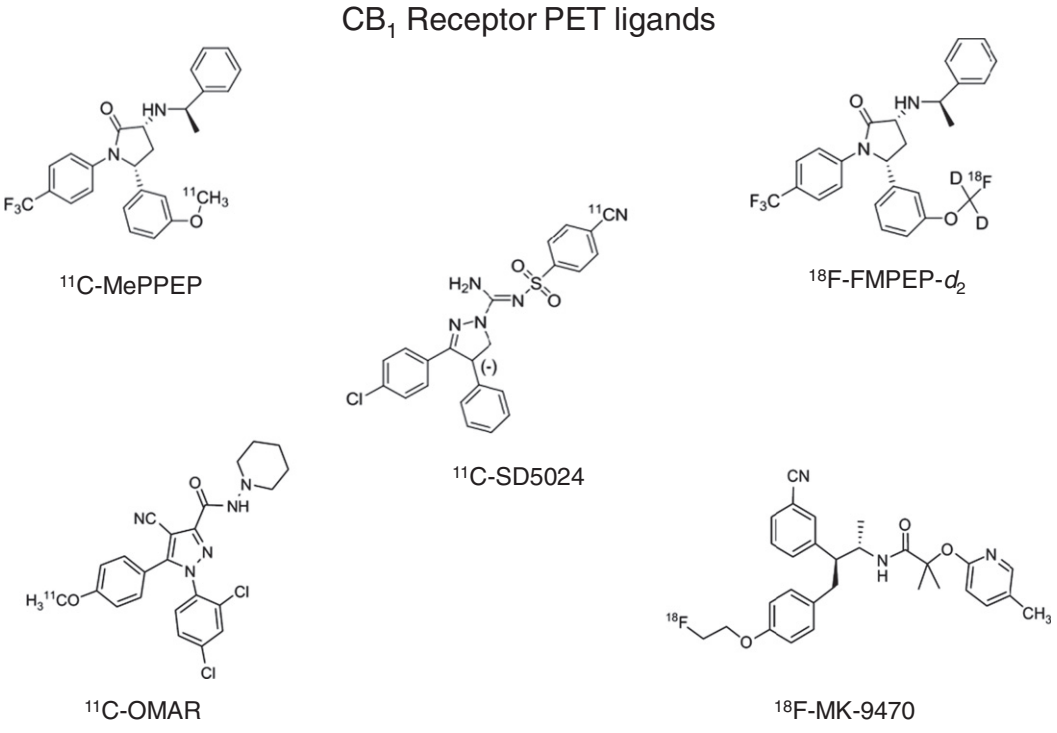

Fig. 1. Chemical structures of five PET ligands for CB_1 receptor.

Radioactivity was measured with liquid scintillation counting for 5 min using 4 mL of Ultima-Gold (Perkin Elmer, Chicago, IL).

Data were analyzed for K_i and IC_{50} using nonlinear regression curve-fitting software provided by GraphPad Prism 5 (GraphPad Software, San Diego, CA, USA). The K_D for MePPEP, 0.31 nM (Jenko et al., 2012), was used in the determination of K_i.

Lipophilicity

The value of $LogD_{7.4}$ was measured at room temperature as previously described (Briard et al., 2008; Zoghbi et al., 1997, 2012). In brief, approximately 22–170 MBq of ^{11}C-MePPEP and 26 MBq of ^{18}F-FMPEP-d_2 (radiochemical purities > 99.6%) were separately added to each of six tubes in 1.0 mL of 0.15 M sodium phosphate buffer (pH 7.4). To each of the test tubes, a 1.0 mL of n-octanol was added and the contents of each test tube were vortexed for 1.0 min. The tubes were then centrifuged at 1800 *g* for 1.0 min after which the two phases were separated and aliquots (200 μL, each) from each phase were counted in an automatic γ-counter. The counts of the aqueous phase were then corrected using the results of the radio-HPLC analysis of the aqueous phases. The average measured $LogD_{7.4}$ was then calculated according to the formula:

$$LogD_{7.4} = \log\left(\frac{cpm\ \ organic\ \ phase}{corrcted\ \ cpm\ \ aqueous\ \ phase}\right)_{7.4}.$$

Samples that contained high levels of radioactivity, outside the optimal sensitivity range of the counter, were allowed to decay until the dead time factor of the counter became normal. Samples with low counts, usually the aqueous phases, were counted first and their measured counting errors (SD/mean) were 4.6% ± 0.3%, 1.8% ± 0.2%, and 0.8% ± 0.07% ($n = 6$ for each) for ^{11}C-MePPEP, ^{18}F-FMPEP-d_2, and ^{11}C-SD5024, respectively.

Monkey PET

Radioligand preparation

^{11}C-SD5024 was prepared from ^{11}C-cyanide ion as labeling agent (Donohue et al., 2008) as detailed in the Investigational New Drug Application (112094) submitted to the U.S. Food and Drug Administration and which is now available at: http://pdsp.med.unc.edu/snidd/. The radioligand was obtained with high radiochemical purity (99.7%) and a specific activity of 41 ± 31 GBq/μmol at times of injection ($n = 4$ batches).

Animals. Two male rhesus monkeys (*Macaca mulatta*; mean weight ± SD, 7.4 ± 4.2 kg) were immobilized with ketamine (10 mg/kg intramuscularly), intubated, and subsequently anesthetized with isoflurane (1%–3% in O_2). Electrocardiograph, body temperature, heart rate, and respiration rate were monitored throughout the experiment. Body temperature was maintained between 36.5 °C and 39.0 °C. All animal experiments were performed in accordance with the Guide for the Care and Use of Laboratory Animals (National Academy Press, 1996) and were approved by the National Institute of Mental Health Animal Care and Use Committee.

Scan procedures

To measure specific binding of ^{11}C-SD5024, a pair of baseline and pre-blocked scans were performed in each of two rhesus male monkeys (total of two baseline and two pre-blocked scans; weight, 7.4 ± 4.2 kg), as previously described (Yasuno et al., 2008). For the pre-blocked scans, rimonabant (3 mg/kg) was intravenously administered 20 min before the radioligand. The PET scans were performed on a Focus 220 (Siemens, Knoxville, TN). ^{11}C-SD5024 (159 ± 47 MBq) was intravenously injected over 1 min and dynamic three-dimensional emission scans were acquired for 120 min in 33 frames. PET images were reconstructed with filtered back projection.

Measurement of ^{11}C-SD5024 in the plasma

To determine arterial input function for brain PET scans, blood samples (1 mL each) were drawn from the femoral artery at 15-second intervals until 120 s, followed by 1 mL samples at 3 and 5 min, and 2 mL at 10, 30, 60, 90, and 120 min. After separating plasma from the whole blood, the concentration of parent radioligand was measured using radio-HPLC, as previously described (Zoghbi et al., 2006) except that mobile phase was MeOH:H_2O:Et_3N (75:25:0.1, by volume).

Human PET

Radioligand preparation

^{11}C-SD5024 was prepared as described above. The radiochemical purity was 100%, and the specific activity was 21 ± 10 GBq/μmol at times of injection ($n = 7$ batches).

Human subjects

Approval for this study was obtained from the Combined Neurosciences Institutional Review Board of the National Institute of Mental Health and the Radiation Safety Committee of the National Institutes of Health. Seven healthy volunteers participated in the brain PET scans (3 males, 4 females; 30 ± 6 years of age). All subjects were free of current medical or psychiatric illnesses.

Measurement of ^{11}C-SD5024 in the plasma

To determine arterial input function for brain PET scans, blood samples (1.5 mL each) were drawn from the radial artery at 15-second intervals until 150 s, followed by 3 mL samples at 3, 4, 6, 8, 10, 15, 20, 30, 40, and 50 min, and 5 mL at 60, 75, 90, and 120 min. The concentration of parent radioligand was measured using HPLC as described above for monkey studies.

Scan procedures

All PET scans were performed on an Advance tomograph (GE Medical Systems, Waukesha, WI). ^{11}C-SD5024 (418 ± 177 MBq) was intravenously injected over 1 min, and dynamic three-dimensional emission scans were acquired for 120 min in 33 frames. Head movement was corrected after the scan by realigning all frames from each subject using Statistical Parametric Mapping, SPM (Version 8 for Windows, Wellcome Department of Cognitive Neurology, UK). The position of the transmission scan was corrected for motion before applying attenuation correction. PET images were reconstructed with filtered back projection.

Data analysis

Blood data processing

For monkey scans, the time-activity curves of ^{11}C-SD5024 concentrations in arterial plasma were fitted to a tri-exponential function.

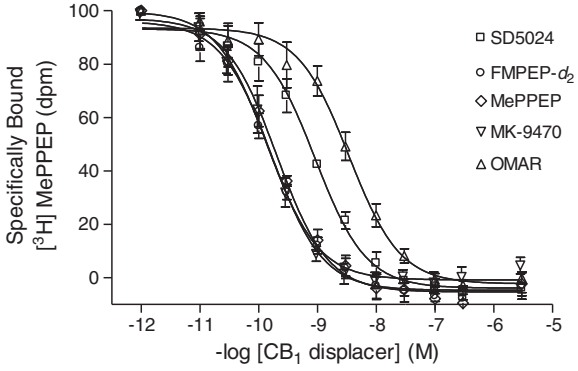

Fig. 2. Displacement curves of ^{3}H-MePPEP by five CB_1 ligands in human parietal cortex homogenate. SD5024 (□), FMPEP-d_2 (○), MePPEP (◇), MK-9470 (▽), OMAR (△). Data represent mean ± 95% confidence interval in nM ($n = 6$).

Table 1
In vitro K_i of CB_1 receptor ligands measured in the human parietal cortex.

Ligand	K_i (nM)	95% CI (nM)
MK-9470	0.10	0.09–0.11
MePPEP	0.11	0.10–0.12
FMPEP-d_2	0.11	0.10–0.13
SD5024	0.47	0.42–0.54
OMAR	2.05	1.82–2.32

Data represent mean and 95% confidence interval (CI) in nM ($n = 6$).

^{11}C-SD5024 concentrations were calculated by multiplying the total plasma activity with fractions of ^{11}C-SD5024 in the total activity of plasma. The tri-exponential fitting was performed by weighting data according to errors in the measurement of each sample. The error levels were estimated from counts without decay correction of each of total plasma activity (A below) and fraction of ^{11}C-SD5024 (B below) based on Poisson distribution and by using the following general formula of propagation of errors.

$$f = AB, \quad \text{variance} = \left(\frac{\sigma_f}{f}\right)^2 \approx \left(\frac{\sigma_A}{A}\right)^2 + \left(\frac{\sigma_B}{B}\right)^2 + 2\frac{\sigma_A \sigma_B}{AB}\rho_{AB}$$

where A and B: actual radioactivity counts, σ_A and σ_B: standard deviations, and ρ_{AB}: correlation coefficient. Fitting was not performed for each of total plasma activity and fraction of ^{11}C-SD5024 as we did for human data (see below) because tri-exponential fitting for the former did not converge and bi-exponential fitting showed marked deviations from the measured values. Radioactivity of the whole blood was used to correct activity in the brain that represented the vasculatures after linear interpolations between the measurements.

For human scans, the time-activity curves of ^{11}C-SD5024 concentrations in arterial plasma were calculated after fitting both total plasma radioactivity and fraction of parent radioligand. The time-activity curves of total radioactivity in each of the plasma and whole blood were fitted to a tri-exponential function by weighting according to the actual radioactivity counts. The fractions of ^{11}C-SD5024 measured in the plasma samples were fitted to a Hill function with Poisson weighting of area-under-the-curve (AUC) of parent peaks from the radio-HPLC.

Image processing

For both monkey and human PET, regional radioactivity was obtained by using a set of preset volumes of interest and MRI coregistered to PET (Tzourio-Mazoyer et al., 2002; Yasuno et al., 2002). Regional data for the following 10 regions were obtained: frontal, parietal, occipital, temporal, and medial temporal cortices; caudate; putamen; cingulate; thalamus; and cerebellum. Realignment, coregistration, and spatial normalization were performed using SPM8. The regional and kinetic analyses were performed using pixelwise modeling software (PMOD 3.16, PMOD Technologies Ltd., http://www.pmod.com/).

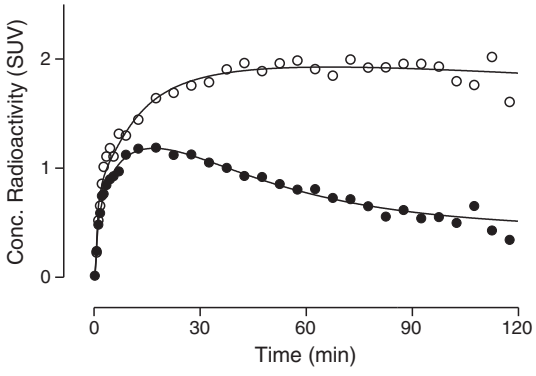

Fig. 3. Brain time activity curves from striatum after intra-venous injection of ^{11}C-SD5024 in a rhesus male monkey (weight; 10.3 kg) under baseline and pretreatment conditions: baseline (o), pretreatment (●). Receptor binding was blocked by pretreatment with intra-venous administration of rimonabant (3 mg/kg). Line represents one tissue compartmental fitting.

Table 2
Regional V_T and specific binding of [^{11}C]SD5024 in two monkey brains.

Region	V_T(mL·cm^{-3})		Specific binding (%)
	Baseline	Preblocked	
Frontal ctx	1.77	0.37	79
	3.13	0.87	72
Parietal ctx	1.39	0.27	81
	2.70	0.69	74
Occipital ctx	1.07	0.24	78
	2.00	0.58	71
Lateral temporal ctx	1.32	0.25	81
	2.52	0.59	77
Medial temporal ctx	1.33	0.39	71
	2.54	0.75	71
Cingulate	1.74	0.27	84
	3.58	0.64	82
Caudate	1.62	0.30	82
	2.79	0.60	79
Putamen	1.84	0.31	83
	3.04	0.56	81
Thalamus	0.83	0.30	64
	1.85	0.59	68
Cerebellum	1.27	0.27	79
	2.34	0.51	78

Specific binding was calculated by (V_T baseline − V_T preblocked) / V_T baseline × 100%.

Calculation of distribution volume

Distribution volume (V_T) is an index of receptor density and equals the ratio at equilibrium of the concentration of radioligand in tissue to that in the plasma. The concentration of radioligand in tissue represents the sum of specific binding (receptor-bound) and non-displaceable uptake (nonspecifically bound and free radioligand in tissue water) (Innis et al., 2007).

Compartmental modeling. Brain time-activity data were analyzed with both one- and unconstrained two-tissue compartment models. Rate constants (K_1, k_2, k_3, and k_4) and percentage of vascular compartment in tissue volume (vB) in standard one- and two-tissue compartment models were estimated with the weighted least-squares method and the Marquardt optimizer. Brain data for each frame were weighted by assuming that the standard deviation/mean of the data was proportional to the inverse square root of noise equivalent counts. The delay between the arrival of ^{11}C-SD5024 in the radial artery and brain was estimated by fitting the whole brain, excluding the white matter.

Because in vitro studies showed that no brain region lacks CB_1 receptor expression (Glass et al., 1997; Herkenham et al., 1990), we did not apply a reference region method in the kinetic analysis.

Time stability

In human studies, to determine the minimal scan length for reliable measurements and also to indirectly assess whether ^{11}C-SD5024 radiometabolites enter the brain, time stability of V_T was examined by increasingly truncating the 120-min scan by 10-minute increments to the shortest length of 0 to 40 min.

Statistical analysis

The optimal compartment model (i.e., one- vs. two-tissue compartments) was chosen based on the Akaike information criterion (AIC),

model selection criterion (MSC proposed by Micromath®, Saint Louis, MO, http://www.micromath.com/products.php?p=scientist&m=statistical_analysis), and *F*-test. The more appropriate model is the one with the smaller AIC and the larger MSC value. *F*-statistics were used to compare goodness-of-fit by one- and two-tissue compartment models. A value of $p < 0.05$ was considered significant. The identifiability (%) of vascular component and rate constants was expressed as a percentage and equaled the ratio of the standard error (SE) of the kinetic variables divided by the value of the kinetic variables themselves. Identifiability (%) of V_T was calculated from the covariance matrix using the generalized form of error propagation equation (Bevington and Robinson, 2003), where correlations among parameters (K_1 and k_2, or K_1, k_2, k_3, and k_4) were taken into account. A lower percentage indicates better identifiability.

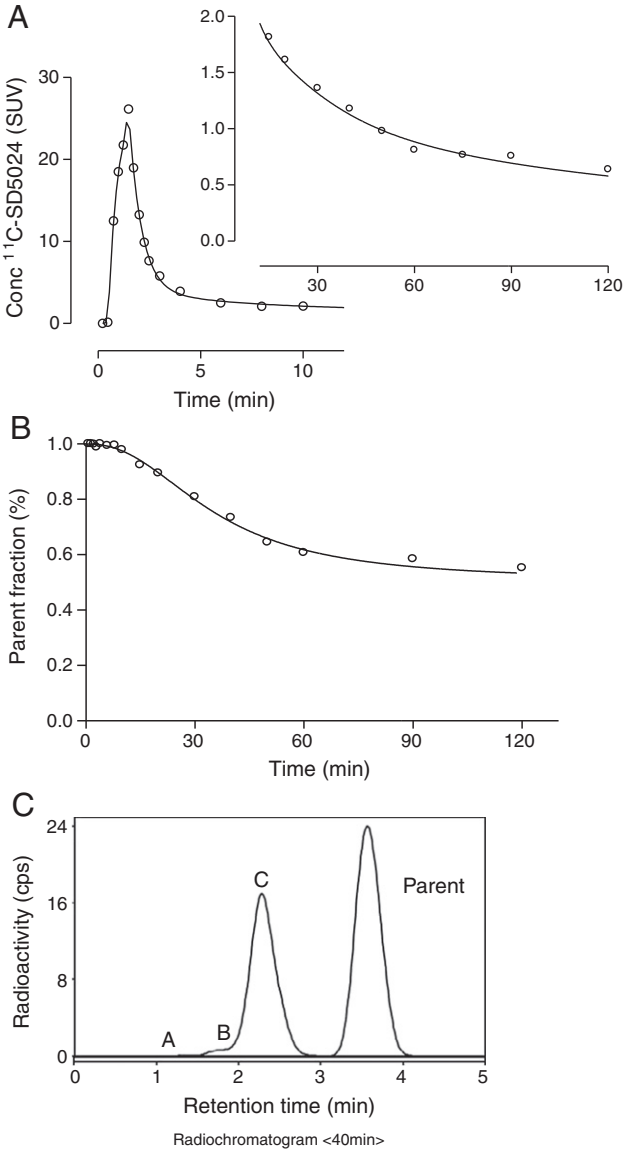

Fig. 4. Radioactivity concentrations, parent radioligand fraction, and radiometabolite profile in the plasma from 31-y-old healthy female subject injected with 277 MBq of ^{11}C-SD5024. (A) Time-course of parent ^{11}C-SD5024 concentration (o) in arterial plasma fitted (−) by multiplying tri-exponential fitted total plasma radioactivity and Hill function fitted plasma parent fraction. (B) Fraction of the unchanged parent radioligand^{11}C-SD5024 (o) in the plasma fitted by a Hill function (−). (C) The radiochromatogram illustrates plasma composition 40 min after injection of ^{11}C-SD5024. Radioactivity was measured in counts per second (cps). Radiometabolite peaks A to C and parent are labeled with increasing lipophilicity.

All statistical analyses were performed using SPSS (Version 17 for Windows, SPSS Inc. Chicago, IL). Group data are expressed as mean ± SD.

Results

In vitro experiments

Binding assay

All five CB_1 receptor ligands showed the presence of one, but not two, binding sites in the inhibition curves of ^{3}H-MePPEP (Fig. 2). Three ligands (FMPEP-d_2, MePPEP, and MK-9470) had high affinity of 0.10 to 0.11 nM (Table 1). OMAR had comparatively low affinity (~2 nM), and SD5024 had intermediate affinity (0.47 nM).

Lipophilicity

The measured lipophilicity index, $LogD_{7.4}$, of ^{11}C-SD5024 (3.79 ± 0.09) was markedly lower than that of ^{11}C-MePPEP (4.77 ± 0.27) and moderately lower than that of ^{18}F-FMPEP-d_2 (4.24 ± 0.08; 6 measurements for each ligand). That is, a difference of one log unit (3.8 vs. 4.8) reflects a ten-fold difference in lipophilicity.

Monkey PET

Brain radioactivity and kinetic analysis

Following injection of ^{11}C-SD5024, brain activity increased to moderate levels (~2 SUV) at ~60 min followed by slow washout (Fig. 3). The distribution of activity was consistent with binding to CB_1 receptors, with high levels in the striatum and low levels in the thalamus. The brain uptake of ^{11}C-SD5024 was markedly reduced with receptor saturating dose of rimonabant (3 mg/kg i.v.) (Fig. 3).

For the kinetic analysis, one-tissue compartmental fitting of time-activity curves converged in all regions and in all scans, but unconstrained two-tissue compartmental fitting did not converge in 11 of 64 fittings in 4 scans. An *F*-test showed that the two-compartment model did not significantly improve goodness-of-fit compared to one-compartment model in 42 of 53 fittings where the two-compartment model converged. The one-compartment model well identified V_T with average SE across brain regions of 3.8%. Regional V_T values ($mL \cdot cm^{-3}$) measured from two monkeys under baseline condition were consistent with the regional rank order of V_T values in the monkey brain previously reported by using ^{11}C-MePPEP (Yasuno et al., 2008), showing high level in the putamen, medium in the lateral temporal cortex, and low in the thalamus (Table 2).

Human PET

Pharmacological effects

The injected mass dose of ^{11}C-SD5024 was 242 ± 47 pmol/kg ($n = 7$), which caused no pharmacological effects, based on subjective reports, vital signs, and laboratory tests.

Plasma analysis

^{11}C-SD5024 concentrations in arterial plasma peaked to 24 ± 8 SUV at 75 s after ^{11}C-SD5024 injection, and then rapidly declined to a slow terminal clearance phase (Fig. 4A). The fraction of ^{11}C-SD5024, expressed as a percentage of total plasma radioactivity, declined slowly and remained 51 ± 13% even at 75 min (Fig. 4B). The fitting of whole blood and total plasma curves converged by tri-exponential function (not shown), and that of parent fraction curve converged by a Hill function in all subjects. Multiplication of fraction of parent (Fig. 4B) and total plasma activity provided ^{11}C-SD5024 concentrations in arterial plasma (Fig. 4A).

Radiometabolites appeared slowly in the plasma and became the predominant component of plasma radioactivity after 90 min. All radiometabolites eluted before the more lipophilic parent by reverse-phase HPLC (Fig. 4C). The parent radioligand eluted at 3.5 min and was well separated from the radiometabolites.

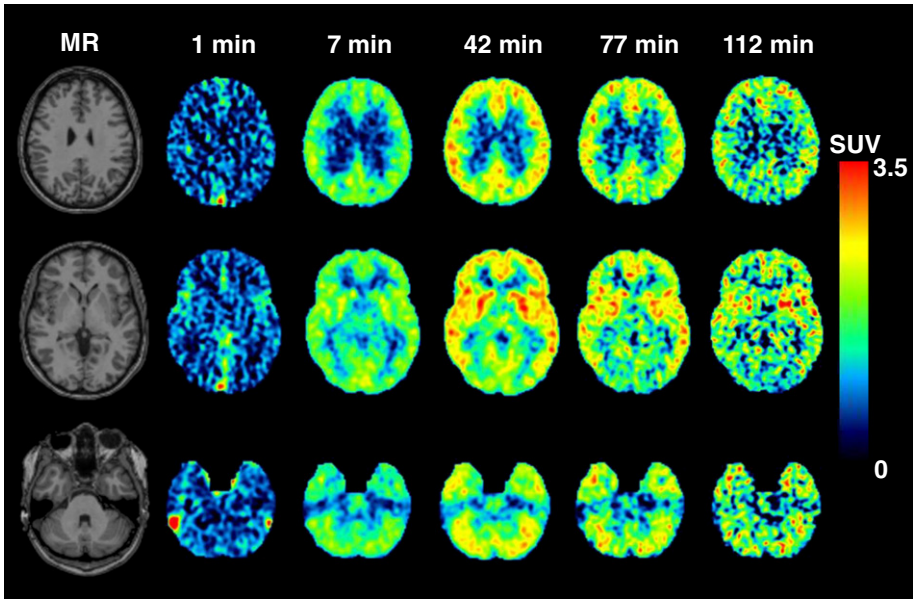

Fig. 5. Magnetic resonance (MR) and dynamic positron emission tomography (PET) images of 31-y-old healthy female subject injected with 277 MBq of ^{11}C-SD5024: MR anatomic images at the levels of centrum semiovale (top row), nucleus basalis (middle row), and pedunculus cerebellaris medius (bottom row) and corresponded PET images obtained at 1, 7, 42, 77, 112 min after tracer injection (from right to left). Each PET image represents standard uptake value (SUV) and is indicated in the SUV color scale on the right.

Brain radioactivity and kinetic analysis

After ^{11}C-SD5024 injection, activity peaked at a moderate concentration (SUV = 1.5–3) at ~40 min, followed by slow washout in all brain regions (Figs. 5, 6). That is, brain radioactivity decreased by only 20% from peak time (40 min) to the end of the scan (120 min). The brain time-activity curves showed a transient and early peak at about 1 min (Fig. 6A). After subtracting activity of vasculature from that of brain regions, this early peak disappeared (Fig. 6B). Thus, this early peak reflected transiently high concentrations of radioactivity in the blood.

Kinetic analysis of brain and plasma data had three major results: 1) Brain uptake was better fit by one- than two-tissue-compartment model, consistent with the majority of brain uptake being specific binding as found in monkey (Table 2). 2) Only the initial 80 min of scan data was adequate to stably measure V_T. 3) The intersubject variability of V_T was low, suggesting that ^{11}C-SD5024 provided relatively precise measurements.

First, one-compartmental fitting converged in all regions and in all scans, but unconstrained two-compartmental fitting did not converge in 31 of 70 fittings in 7 scans. This result is consistent with the majority of brain uptake having one kinetic profile — i.e., the predominant uptake being in the specific (i.e., receptor-bound) compartment. In addition, in 39 fittings where both one- and two-compartment models converged, the former showed better goodness-of-fit than the latter, based on AIC and MSC scores and the *F*-test. One-compartment model showed lower mean AIC scores (252 vs. 259) and higher mean MSC scores (3.6 vs 3.5) than the unconstrained two-compartment model. An *F*-test showed that the two-compartment model did not significantly improve goodness-of-fit than one-compartment model (Fig. 6A). The one-compartment model well identified V_T with average SE across brain regions of 1.8%. Regional V_T values were consistent with known distribution of CB_1 receptors, showing high level in the putamen, medium in the frontal cortex, and low in the thalamus (Table 3).

Second, despite the moderately slow washout of the radioligand from the brain, only the initial 80 min of scanning provided values of V_T equivalent to that using the complete 120 min of scanning. To determine the minimal scanning time to give accurate V_T, we increasingly truncated the entire scan by 10-min increments from 0–120 to 0–40 min but displayed only half of these intervals (Fig. 7). As expected, short scanning lengths (e.g., 40 and 60 min) overestimated V_T, especially

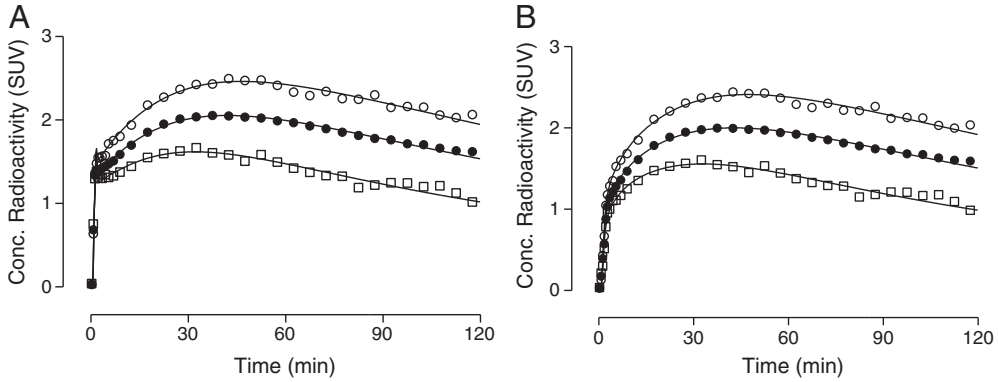

Fig. 6. Representative brain uptake with compartmental fitting from 31-y-old healthy female subject injected with 277 MBq of ^{11}C-SD5024.(A) Concentration of radioactivity from 3 regions is shown: putamen (o), with highest uptake; frontal cortex (●), with medium uptake; and thalamus (□), with lowest uptake. Line represents one-tissue compartmental fitting. For this scan, both one- and two-compartmental fitting converged. Fitted curves by one- and two-compartment models almost overlap and these curves are not visually distinguishable.(B) Vascular component-corrected brain time activity curves. Initial spikes of time activity curve (A) disappeared after subtracting blood activity in brain calculated from percentage of vasculatures in brain and whole blood activity.

Table 3
Parameters measured with one-tissue compartment model in the human brain.

Region	vB (%)	Standard error (%)	K_1 (mL·cm^{-3}·min^{-1})	Standard error (%)	k_2 (/min)	Standard error (%)	V_T (mL·cm^{-3})	Standard error (%)
Frontal	4.4 ± 0.66	4.67	0.032 ± 0.006	0.72	0.013 ± 0.003	2.02	2.57 ± 0.54	1.43
Parietal	4.8 ± 0.50	4.73	0.034 ± 0.006	0.80	0.014 ± 0.003	2.11	2.44 ± 0.50	1.45
Occipital	5.9 ± 0.49	3.94	0.035 ± 0.007	0.87	0.018 ± 0.003	1.96	2.00 ± 0.38	1.26
Lateral temporal	5.2 ± 0.64	4.12	0.032 ± 0.007	0.77	0.012 ± 0.002	2.25	2.66 ± 0.57	1.61
Medial temporal	5.3 ± 0.58	4.22	0.023 ± 0.005	1.05	0.010 ± 0.002	3.58	2.48 ± 0.65	2.69
Cingulate	5.0 ± 0.58	4.94	0.029 ± 0.006	0.94	0.011 ± 0.002	3.05	2.79 ± 0.58	2.27
Caudate	3.7 ± 0.67	7.26	0.028 ± 0.005	1.07	0.013 ± 0.003	3.02	2.31 ± 0.55	2.14
Putamen	4.0 ± 0.79	8.21	0.038 ± 0.008	0.94	0.012 ± 0.003	2.83	3.16 ± 0.70	2.06
Thalamus	4.6 ± 0.49	5.53	0.029 ± 0.006	1.17	0.017 ± 0.004	2.66	1.71 ± 0.41	1.71
Cerebellum	6.4 ± 0.69	3.73	0.030 ± 0.006	1.03	0.016 ± 0.003	2.45	1.93 ± 0.38	1.61

Percentage of vascular compartment in tissue volume (vB), kinetic rate constants (K_1 and k_2) and total distribution volume (V_T) from seven human subjects are shown as mean ± SD. For each brain region, median standard errors are also listed and are expressed as % of the variable itself.

in highest density regions, which are the latest to achieve peak uptake. Scanning for 80 or 100 min provided values which were essentially equivalent to those from 120 min, which is regarded in this analysis as the "correct" value. These results not only show that 80 min of scanning with ^{11}C-SD5024 is adequate to measure CB_1 receptors but also suggest that radiometabolites do not significantly accumulate in the brain. That is, brain uptake was fully and stably defined by 80 min from the input function of only the parent radioligand in the plasma.

As background to the third result, we previously found that ^{11}C-MePPEP had high intersubject variability (~60%), which was caused in large part by noise (imprecision) in the measurement of low concentrations of radioligand in the plasma, especially at late time points (Terry et al., 2009). As an indirect measure of precision of ^{11}C-SD5024, intersubject variability of V_T was small and had an average value of 22%. This result suggests that ^{11}C-SD5024 provides less noisy (more precise) measurement than ^{11}C-MePPEP.

Comparison on in vivo binding of ^{11}C-SD5024 with that of the other PET ligands

The specific binding of ^{11}C-SD5024 in the monkey brain (measured at baseline and after receptor blockade) was high and represented 71–82% of V_T (mean of two monkey studies, Table 2). Specific binding of ^{11}C-SD5024 was similar to that of ^{11}C-MePPEP and ^{18}F-FMPEP-d_2 (Table 4).

For human studies, we compared ^{11}C-SD5024 and the four other CB_1 radioligands with regard to peak brain uptake (which reflects the magnitude of the brain signal per unit of injected activity), V_T and the intersubject variability of V_T (as an indirect measure of precision) (Tables 5, 6). For the ^{11}C-labeled radioligands, the peak brain uptake of ^{11}C-SD5024 was about 20% lower than that of ^{11}C-MePPEP but about 40% higher than that of ^{11}C-OMAR (Table 5). Based on only brain uptake, ^{11}C-SD5024 appears superior to ^{11}C-OMAR, but the actual impact on quantitation of V_T also depends on reproducibility of both plasma and brain measurements. ^{11}C-SD5024 showed about twice higher V_T values than ^{11}C-OMAR, but V_T of ^{11}C-SD5024 was only 15–20% of that for ^{18}F-MK-9470, ^{11}C-MePPEP, and ^{18}F-FMPEP-d_2 (Table 6). Greater V_T values may reflect higher levels of in vivo affinity. However, the presence of two unknown parameters should be noted: nondisplaceable distribution volume and the free fraction in the plasma (f_P) (see Discussion) (Innis et al., 2007).

^{11}C-SD5024 showed low intersubject variability (~24%) for V_T (Table 6), indicating good precision. The intersubject variability of ^{11}C-SD5024, ^{11}C-OMAR, and ^{18}F-FMPEP-d_2 was markedly smaller than

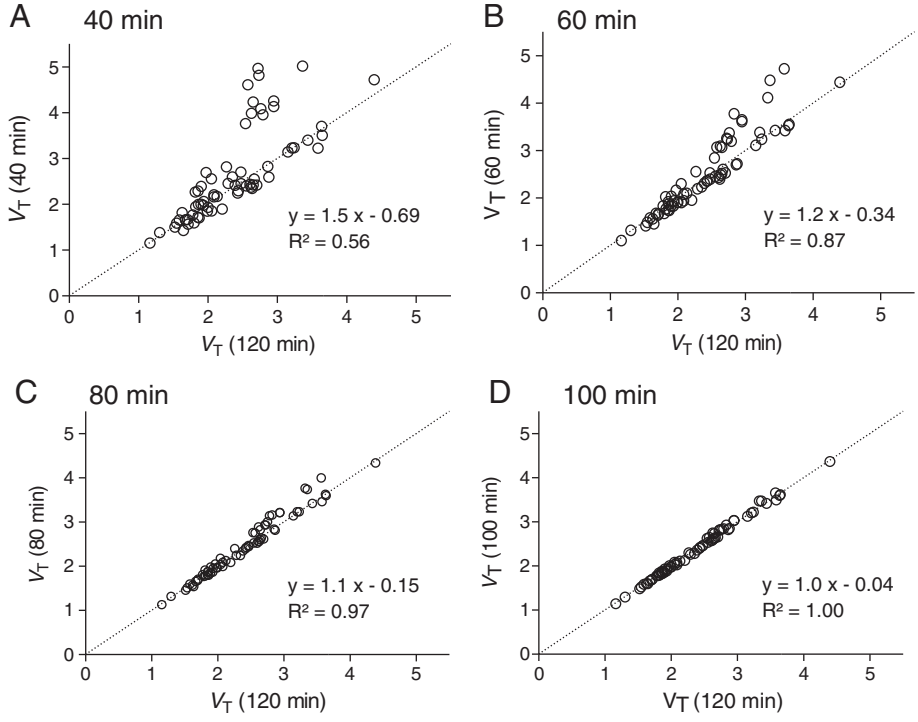

Fig. 7. Effect of increasing scan duration on total distribution volume (V_T) determined with a one-tissue compartment model. Correlation between V_T calculated from the complete 120 min of scanning (*x*-axis) and that calculated from the initial (A) 40, (B) 60, (C) 80, or (D) 100 min of scanning (*y*-axis). The dots represent 70 regions from 7 subjects. The dotted line in each graph is the line of identity.

Table 4
Comparison of specific binding of three CB_1 receptor ligands in the monkey brain.

Radioligand	V_T (mL·cm^{-3}, striatum)		Specific binding(%)
	Baseline	Preblocked	
^{11}C-MePPEP [a]	24.3	2.9	88
^{18}F-FMPEP-d_2 [a]	35.4	5.4	85
^{11}C-SD5024	2.36	0.44	82

For comparison, values of V_T in striatum were used, which were previously reported. V_T values in striatum of ^{11}C-SD5024 were calculated from those in caudate and putamen (Table 2). Specific binding was calculated by (V_T baseline − V_T preblock) / V_T baseline × 100%.
[a] Terry et al. (2010).

that of ^{11}C-MePPEP (~60%) and ^{18}F-MK-9470 (~66%) with the smallest variability for ^{11}C-OMAR.

Although the spread (intersubject variability) of V_T may provide an indirect measure of precision, the absolute V_T values themselves can be misleading when comparing radioligands. For example, the V_T values of ^{11}C-SD5024 were about two-fold greater than those of ^{11}C-OMAR, which may merely parallel differences in f_P. A more valid comparison would normalize V_T for f_P, but the f_P values of ^{11}C-OMAR have not been reported.

Discussion

We evaluated a new ^{11}C-labeled compound, ^{11}C-SD5024, to quantify CB_1 receptors based on its in vitro and in vivo characteristics. SD5024 ($LogD_{7.4} = 3.8$) has lipophilicity more appropriate than that of MePPEP (4.8) and FMPEP (4.2) for brain imaging (Waterhouse, 2003). The intermediate affinity ($K_i = 0.47$ nM) may be appropriate to image the high density target. ^{11}C-SD5024 had a high percentage (~80%) of specific binding in the monkey brain. In humans, ^{11}C-SD5024 was well quantified with a one-compartment model and only 80 min of scan data. ^{11}C-SD5024 had a similarly low intersubject variability as that for ^{18}F-FMPEP-d_2. Taken together, our results show that ^{11}C-SD5024 is a promising ligand to image CB_1 receptors in humans. It is clearly better than ^{11}C-MePPEP (which we previously studied) and may be slightly better than or equivalent to ^{11}C-OMAR (which was studied at another institution). Human studies of retest variability and of receptor blockade are needed to conclude which ^{11}C-labeled ligand is the best to image CB_1 receptors.

One limitation of the current study with regard to comparing radioligands is that we did not have 'head-to-head' comparisons in the same or similar subjects. Nevertheless, our direct experience with three of the radioligands (^{11}C-SD5024, ^{11}C-MePPEP, and ^{18}F-FMPEP-d_2) and the knowledge of the difficulties associated with imaging a high density target like the CB_1 receptor allow some certainty in our speculations. For example, the CB_1 receptor is one of the most abundant G-protein-coupled receptors with high density in the brain (Katona and Freund, 2008; Wilson and Nicoll, 2002). As such, high localized density of these targets will slow the washout of radioligand from the brain. The radioligand is thought to bind and re-bind to the receptor before moving to the free compartment of the brain and be available for transfer into the blood (Frost and Wagner, 1984; Innis et al., 2007). This so-called "synaptic compartment" makes it difficult to accurately measure the in vivo dissociation rate constant (k_4) and the erroneously measured k_4 is dependent on receptor density (B_{max}) due to errors. The affinity of a radioligand, especially for a high density target, may well be so high that washout from the brain cannot be reliably measured during the scanning period allowed by the half-life of the radionuclide. Thus, for the ^{11}C-labeled radioligands for the CB_1 receptor, the high affinity of ^{11}C-MePPEP (0.11 nM) contributes to its slow washout from the brain and suggests that the lower affinities of ^{11}C-SD5024 (0.47 nM) and ^{11}C-OMAR (2.05 nM; Table 1) are more appropriate.

We previously compared ^{11}C-MePPEP and ^{18}F-FMPEP-d_2 in a similar group of healthy subjects using a retest paradigm (Terry et al., 2009, 2010). The purpose of that study was to determine the causes of the large intersubject variability of ^{11}C-MePPEP compared to ^{18}F-FMPEP-d_2 when we did not know the actual variation in receptor density in the study population. Because distribution volume (V_T) is a ratio of concentration of radioactivity in the brain to that in the plasma, the retest paradigm allowed identification with moderate certainty of the relative contributions of measurement errors (noise) in the calculation of V_T. That study somewhat surprisingly showed that the errors in measuring the concentrations of radioligand in the plasma were more problematic to calculate V_T than measuring radioligand in the brain. That is, the large intersubject variability of V_T using ^{11}C-MePPEP was largely caused by the poor precision in the measurement of low concentrations of radioligand in the plasma, particularly at late time points (Terry et al., 2009, 2010). The current study of ^{11}C-SD5024 may have achieved a more accurate arterial input function than that of ^{11}C-MePPEP because the plasma concentrations of ^{11}C-SD5024 were much higher than those of ^{11}C-MePPEP. For example, the plasma concentrations from 30 to 120 min of ^{11}C-SD5024 were five-times that of ^{11}C-MePPEP (Fig. 4A and Terry et al., 2009).

Our prior comparison of ^{11}C-MePPEP and ^{18}F-FMPEP-d_2 showed the utility of a retest paradigm to identify contributors to the intersubject variability of V_T from noisy (imprecise) measurements in the brain and plasma. In the absence of a retest paradigm (as in the current study), intersubject variability by itself is merely an indirect measurement of precision. For example, the large intersubject variability reported for one radioligand may reflect the actual biological variability in a diverse study population. Nevertheless, our experience with comparison of ^{11}C-MePPEP and ^{18}F-FMPEP-d_2 showed that large intersubject variability of V_T suggests, but does not prove, relatively noisy measurements in either the brain or plasma.

Specific binding in human, i.e., V_S/f_P, has not been measured for any of the five CB_1 ligands. Nevertheless, based on currently available data of indirect measures of specific binding, i.e., V_T and peak brain uptake in human, ^{11}C-SD5024 appears to be slightly better than ^{11}C-OMAR. To determine which ^{11}C-labeled ligand is the best, particularly for the comparison between ^{11}C-SD5024 and ^{11}C-OMAR, receptor occupancy studies in human are required where specific binding is measured by comparing V_T/f_P under baseline and receptor blockade. Because f_P is too low to measure accurately for ^{11}C-SD5024 or not reported for ^{11}C-OMAR, currently, V_T and peak brain uptake in human (Table 5, 6) are the most useful parameters to compare ^{11}C-SD5024 and ^{11}C-OMAR. Although peak uptake is a crude parameter, it may reflect how much free ligand enters the brain and binds to the receptor. ^{11}C-SD5024 showed ~1.4 times greater peak brain uptake (Table 5) and about twice greater V_T (Table 6) than ^{11}C-OMAR. These human PET data are in line with the results of the in vitro experiments where SD5024 showed four times greater affinity than OMAR (Table 1). However, a comparison based on V_S/f_P is still needed.

Conclusions

^{11}C-SD5024 showed appropriate lipophilicity, high specific binding in the monkey brain, and good precision for measuring CB_1 receptors in humans. ^{11}C-SD5024 is, therefore, a promising ligand to image CB_1

Table 5
Comparison of peak uptake (SUV) in putamen among five CB_1 receptor ligands.

Radioligand	Peak uptake (SUV) in putamen
^{11}C-SD5024	1.7–3.0
^{11}C-MePPEP [a]	3–4
^{18}F-FMPEP-$d2$ [b]	3–4
^{18}F-MK-9470 [c]	1.3–1.7
^{11}C-OMAR [d]	1.4–2.1

[a] Terry et al. (2009).
[b] Terry et al. (2010).
[c] Burns et al. (2007), Sanabria-Bohórquez et al. (2010).
[d] Wong et al. (2010).

Table 6
Comparison of V_T and intersubject variability (SD/mean) among five CB_1 receptor ligands.

^{11}C-labeled ligands						^{18}F-labeled ligands					
Region	^{11}C-OMAR[a] (n = 10, 90 min)		Region	^{11}C-MePPEP[b] (n = 17, 150 min)		^{11}C-SD5024 (n = 7, 120 min)		^{18}F-FMPEP-d_2[c] (n = 9, 120 min)		^{18}F-MK-9470[d] (n = 12, 700, 360, 150 min)	
	V_T (mL·cm^{-3})	Intersubject variability		V_T (mL·cm^{-3})	Intersubject variability	V_T (mL·cm^{-3})	Intersubject variability	V_T (mL·cm^{-3})	Intersubject variability	V_T (mL·cm^{-3})	Intersubject variability
Globus pallidus	1.47 ± 0.25	17%	Frontal	22.4 ± 12.8	57%	2.57 ± 0.54	21%	22.7 ± 6.4	28%	22.4 ± 13.1	58%
Cingulate	1.23 ± 0.16	13%	Thalamus	11.2 ± 5.0	44%	1.71 ± 0.41	24%	9.6 ± 2.5	26%	12.6 ± 7.6	60%
Putamen	1.32 ± 0.20	15%	Putamen	29.1 ± 17.4	60%	3.15 ± 0.70	22%	24.3 ± 7.2	29%	25.1 ± 13.3	53%

Values of V_T are shown as mean ± SD and intersubject variability is calculated by SD / mean.
[a] Wong et al. (2010).
[b] Terry et al. (2009).
[c] Terry et al. (2010).
[d] Sanabria-Bohórquez et al. (2010).

receptors and appropriate for patient studies. Among the three ^{11}C-labeled ligands, SD5024 is clearly superior to MePPEP and may be slightly better or equivalent to OMAR. However, additional human studies of retest reproducibility and receptor blockade would be necessary to determine whether one is clearly superior to the other.

Acknowledgments

This study was supported by the Intramural Research Program of the National Institute of Mental Health, National Institutes of Health (IRP-NIMH-NIH) and by the 2011/2013 Wagner-Torizuka Fellowship of Society of Nuclear Medicine. We thank Maria Ferraris Araneta, Denise Rallis-Frutos, Gerald Hodges, David Clark, Jeih-San Liow, and the staff of the PET Department for assistance in successful completion of the studies, and PMOD Technologies (Zurich, Switzerland) for providing its image analysis and modeling software. We thank Andrew Horti (Johns Hopkins) for providing a sample of OMAR and Terence Hamill (Merck Research Laboratories) for providing a sample of MK-9470.

Conflict of interest statement

There are no conflicts of interest.

References

Bevington, P.R., Robinson, D.K., 2003. Data Reduction and Error Analysis for the Physical Sciences, 3rd edition. McGraw-Hill, Boston.
Briard, E., Zoghbi, S.S., Imaizumi, M., Gourley, J.P., Shetty, H.U., Hong, J., Cropley, V., Fujita, M., Innis, R.B., Pike, V.W., 2008. Synthesis and evaluation in monkey of two sensitive ^{11}C-labeled aryloxyanilide ligands for imaging brain peripheral benzodiazepine receptors in vivo. J. Med. Chem. 51, 17–30.
Burns, H.D., Van Laere, K., Sanabria-Bohórquez, S., Hamill, T.G., Bormans, G., Eng, W.S., Gibson, R., Ryan, C., Connolly, B., Patel, S., Krause, S., Vanko, A., Van Hecken, A., Dupont, P., De Lepeleire, I., Rothenberg, P., Stoch, S.A., Cote, J., Hagmann, W.K., Jewell, J.P., Lin, L.S., Liu, P., Goulet, M.T., Gottesdiener, K., Wagner, J.A., de Hoon, J., Mortelmans, L., Fong, T.M., Hargreaves, R.J., 2007. [^{18}F]MK-9470, a positron emission tomography (PET) tracer for in vivo human PET brain imaging of the cannabinoid-1 receptor. Proc. Natl. Acad. Sci. U. S. A. 104, 9800–9805.
Donohue, S.R., Pike, V.W., Finnema, S.J., Truong, P., Andersson, J., Gulyás, B., Halldin, C., 2008. Discovery and labeling of high-affinity 3,4-diarylpyrazolines as candidate radioligands for in vivo imaging of cannabinoid subtype-1 (CB_1) receptors. J. Med. Chem. 51, 5608–5616.
Eggan, S.M., Hashimoto, T., Lewis, D.A., 2008. Reduced cortical cannabinoid 1 receptor messenger RNA and protein expression in schizophrenia. Arch. Gen. Psychiatry 65, 772–784.
Frost, J.J., Wagner Jr., H.N., 1984. Kinetics of binding to opiate receptors in vivo predicted from in vitro parameters. Brain Res. 305, 1–11.
Gazzerro, P., Caruso, M.G., Notarnicola, M., Misciagna, G., Guerra, V., Laezza, C., Bifulco, M., 2007. Association between cannabinoid type-1 receptor polymorphism and body mass index in a southern Italian population. Int. J. Obes. (Lond). 31, 908–912.
Glass, M., Dragunow, M., Faull, R.L., 1997. Cannabinoid receptors in the human brain: a detailed anatomical and quantitative autoradiographic study in the fetal, neonatal and adult human brain. Neuroscience 77, 299–318.
Herkenham, M., Lynn, A.B., Little, M.D., Johnson, M.R., Melvin, L.S., de Costa, B.R., Rice, K.C., 1990. Cannabinoid receptor localization in brain. Proc. Natl. Acad. Sci. U. S. A. 87, 1932–1936.
Innis, R.B., Cunningham, V.J., Delforge, J., Fujita, M., Gjedde, A., Gunn, R.N., Holden, J., Houle, S., Huang, S.C., Ichise, M., Iida, H., Ito, H., Kimura, Y., Koeppe, R.A., Knudsen, G.M., Knuuti, J., Lammertsma, A.A., Laruelle, M., Logan, J., Maguire, R.P., Mintun, M.A., Morris, E.D., Parsey, R., Price, J.C., Slifstein, M., Sossi, V., Suhara, T., Votaw, J.R., Wong, D.F., Carson, R.E., 2007. Consensus nomenclature for in vivo imaging of reversibly binding radioligands. J. Cereb. Blood Flow Metab. 27, 1533–1539.
Jenko, K.J., Hirvonen, J., Henter, I.D., Anderson, K.B., Zoghbi, S.S., Hyde, T.M., Deep-Soboslay, A., Innis, R.B., Kleinman, J.E., 2012. Binding of a tritiated inverse agonist to cannabinoid CB_1 receptors is increased in patients with schizophrenia. Schizophr. Res. 141, 185–188.
Jones, D., 2008. End of the line for cannabinoid receptor 1 as an anti-obesity target? Nat. Rev. Drug Discov. 7, 961–962.
Katona, I., Freund, T.F., 2008. Endocannabinoid signaling as a synaptic circuit breaker in neurological disease. Nat. Med. 14, 923–930.
Matsuda, L.A., Lolait, S.J., Brownstein, M.J., Young, A.C., Bonner, T.I., 1990. Structure of a cannabinoid receptor and functional expression of the cloned cDNA. Nature 346, 561–564.
National Academy Press, 1996. Guide for the Care and Use of Laboratory Animals (Washington, DC.).
Sanabria-Bohórquez, S.M., Hamill, T.G., Goffin, K., De Lepeleire, I., Bormans, G., Burns, H.D., Van Laere, K., 2010. Kinetic analysis of the cannabinoid-1 receptor PET tracer [^{18}F]MK-9470 in human brain. Eur. J. Nucl. Med. Mol. Imaging 37, 920–933.
Terry, G.E., Liow, J.S., Zoghbi, S.S., Hirvonen, J., Farris, A.G., Lerner, A., Tauscher, J.T., Schaus, J.M., Phebus, L., Felder, C.C., Morse, C.L., Hong, J.S., Pike, V.W., Halldin, C., Innis, R.B., 2009. Quantitation of cannabinoid CB_1 receptors in healthy human brain using positron emission tomography and an inverse agonist radioligand. Neuroimage 48, 362–370.
Terry, G.E., Hirvonen, J., Liow, J.S., Zoghbi, S.S., Gladding, R., Tauscher, J.T., Schaus, J.M., Phebus, L., Felder, C.C., Morse, C.L., Donohue, S.R., Pike, V.W., Halldin, C., Innis, R.B., 2010. Imaging and quantitation of cannabinoid CB_1 receptors in human and monkey brains using ^{18}F-labeled inverse agonist radioligands. J. Nucl. Med. 51, 112–120.
Tzourio-Mazoyer, N., Landeau, B., Papathanassiou, D., Crivello, F., Etard, O., Delcroix, N., Mazoyer, B., Joliot, M., 2002. Automated anatomical labeling of activations in SPM using a macroscopic anatomical parcellation of the MNI MRI single-subject brain. Neuroimage 15, 273–289.
Van Gaal, L.F., Rissanen, A.M., Scheen, A.J., Ziegler, O., Rössner, S., RIO-Europe Study Group, 2005. Effects of the cannabinoid-1 receptor blocker rimonabant on weight reduction and cardiovascular risk factors in overweight patients: 1-year experience from the RIO-Europe study. Lancet 365, 1389–1397.
Waterhouse, R.N., 2003. Determination of lipophilicity and its use as a predictor of blood–brain barrier penetration of molecular imaging agents. Mol. Imaging Biol. 5, 376–389.
Wilson, R.I., Nicoll, R.A., 2002. Endocannabinoid signaling in the brain. Science 296, 678–682.
Wong, D.F., Kuwabara, H., Horti, A.G., Raymont, V., Brasic, J., Guevara, M., Ye, W., Dannals, R.F., Ravert, H.T., Nandi, A., Rahmim, A., Ming, J.E., Grachev, I., Roy, C., Cascella, N., 2010. Quantification of cerebral cannabinoid receptors subtype 1 (CB_1) in healthy subjects and schizophrenia by the novel PET radioligand [^{11}C]OMAR. Neuroimage 52, 1505–1513.
Yasuno, F., Hasnine, A.H., Suhara, T., Ichimiya, T., Sudo, Y., Inoue, M., Takano, A., Ou, T., Ando, T., Toyama, H., 2002. Template-based method for multiple volumes of interest of human brain PET images. Neuroimage 16, 577–586.
Yasuno, F., Brown, A.K., Zoghbi, S.S., Krushinski, J.H., Chernet, E., Tauscher, J., Schaus, J.M., Phebus, L.A., Chesterfield, A.K., Felder, C.C., Gladding, R.L., Hong, J., Halldin, C., Pike, V.W., Innis, R.B., 2008. The PET radioligand [^{11}C]MePPEP binds reversibly and with high specific signal to cannabinoid CB_1 receptors in nonhuman primate brain. Neuropsychopharmacology 33, 259–269.
Zoghbi, S.S., Baldwin, R.M., Seibyl, J.P., Charney, D.S., Innis, R.B., 1997. A radiotracer technique for determining apparent pKa of receptor-binding ligands. J. Label. Compd. Radiopharm. 40SI, 136–138.
Zoghbi, S.S., Shetty, H.U., Ichise, M., Fujita, M., Imaizumi, M., Liow, J.S., Shah, J., Musachio, J.L., Pike, V.W., Innis, R.B., 2006. PET imaging of the dopamine transporter with ^{18}F-FECNT: a polar radiometabolite confounds brain radioligand measurements. J. Nucl. Med. 47, 520–527.
Zoghbi, S.S., Anderson, K.B., Jenko, K.J., Luckenbaugh, D.A., Innis, R.B., Pike, V.W., 2012. On quantitative relationships between drug-like compound lipophilicity and plasma free fraction in monkey and human. J. Pharm. Sci. 101, 1028–1039.